

1 **Enhanced bioavailability of dissolved organic matter (DOM) in human-disturbed**
2 **streams in Alpine fluvial networks**

3 Thibault Lambert^{1,*}, Pascal Perolo¹, Nicolas Escoffier¹, Marie-Elodie Perga¹

4 ¹ Faculty of Geoscience and Environment, Institute of Earth Surface Dynamics, University of
5 Lausanne, Lausanne, Switzerland

6 * corresponding author

7 Thibault Lambert thibault.lambert@unil.ch

8 Pascal Perolo pascal.perolo@unil.ch

9 Nicolas Escoffier nicolas.escoffier@unil.ch

10 Marie-Elodie Perga marie-elodie.perga@unil.ch

11 **Abstract**

12 The influence of human activities on the role of inland waters in the global carbon (C)
13 cycle is poorly constrained. In this study, we investigated the impact of human land use on the
14 sources and biodegradation of dissolved organic matter (DOM) and its potential impact on
15 bacterial respiration in ten independent catchments of the Lake Geneva Basin. Sites were
16 selected along a gradient of human disturbance (agriculture and urbanization) and were visited
17 twice during the winter high flow period. Bacterial respiration and DOM bioavailability were
18 measured in laboratory through standardized dark bioassays, and the influence of human land
19 uses on DOM sources, composition and reactivity was assessed from fluorescence
20 spectroscopy. Bacterial respiration was higher in agro-urban streams but was related to a
21 short-term bioreactive pool (0-6 days of incubation) from autochthonous origin which relative
22 contribution to the total DOM pool increased with the degree of human disturbance. On the
23 other hand, the degradation of a long-term (6-28 days) bioreactive pool related to terrestrial
24 DOM was independent from the catchment land use and did not contribute substantially to
25 aquatic bacterial respiration. From a greenhouse gas emission perspective, our results
26 suggest that human activities may have a limited impact on the net C exchanges between
27 inland waters and the atmosphere, as most CO₂ fixed by aquatic producers in agro-urban
28 streams is cycled back to the atmosphere after biomineralization. Although seasonal and
29 longitudinal changes in DOM sources must be considered, the implications of our results likely
30 apply more widely as greater proportion of autochthonous-DOM signature is a common feature
31 in human-impacted catchments. Yet, on a global scale, the influence of human activities
32 remains to be determined given the large diversity of effects of agriculture and urbanization on
33 freshwater DOM depending on the local environmental context.

34

35 1. Introduction

36 Continental surface waters receive more terrestrial carbon (C) than they export toward
37 oceans, leading to the conceptualization of inland waters as active pipes that process, emit
38 and store C during its transit from lands to oceans (Cole et al., 2007). Within this framework,
39 the mineralization of terrestrial dissolved organic matter (DOM) by aquatic heterotrophic
40 bacterial communities is a key process by which terrestrial C returns to the atmosphere through
41 CO₂ emissions (Fasching et al., 2014; Lapierre et al., 2013; Mayorga et al., 2005). The study
42 of DOM transport and transformation along fluvial networks is therefore of primary importance,
43 yet a major gap in knowledge revolves around the impact of human activities on the reactivity
44 and bacterial use (i.e., respiration or allocation to biomass) of terrestrial DOM in inland waters
45 (Creed et al., 2015; Xenopoulos et al., 2021).

46 Agricultural and urban land uses are major catchment features impacting DOM sources
47 and composition in aquatic ecosystems from local (Wilson and Xenopoulos, 2009) to regional
48 scales (Lambert et al., 2017; Williams et al., 2016). Streams draining agricultural landscapes
49 and/or urban catchments are commonly enriched in DOM of low molecular weight compared
50 to streams draining forested catchments whereby DOM is dominated by aromatic, high
51 molecular weight compounds (Lambert et al., 2017; Williams et al., 2010). Greater proportions
52 of lower molecular weight compounds in agro-urban streams can be the consequence of a
53 greater autochthonous algal production and bacterial activity in nutrient-enriched waters (Fuß
54 et al., 2017; Lu et al., 2014; Williams et al., 2010; Wu et al., 2019), reduced hydrological
55 connection with terrestrial sources (Giling et al., 2014; Parr et al., 2015), or transfer of less
56 humified soil organic matter due to agricultural practices (Humbert et al., 2020; Lambert et al.,
57 2017; Landsman-Gerjoi et al., 2020). As lower molecular weight molecules are typically more
58 labile and easily available for uptake to bacterial communities (Berggren et al., 2010; Catalán
59 et al., 2017; Kaplan and Bott, 1989), greater DOM processing can be expected in agro-urban
60 streams (Hosen et al., 2014; Parr et al., 2015). However, the destabilization of a stock of soil
61 organic material built before the conversion of forests or wetlands for agriculture or urban
62 development can lead to the mobilization of large amounts of humic and highly aromatic DOM
63 into surface waters (Ekblad and Bastviken, 2019; Graeber et al., 2012; Hu et al., 2016; Petrone
64 et al., 2011). As a consequence, the impact of human land uses on the dynamic of DOM in
65 inland waters may be highly diverse depending on how agriculture and urbanization affect
66 DOM sources, content, and composition as well as external drivers such as inorganic nutrients
67 known to regulate bacterial DOM processing (Guillemette and del Giorgio, 2012; Reche et al.,
68 1998).

69 Different scenarios about the consequences on net C exchanges for surface waters
70 can be envisaged depending on the impact of human land uses on freshwater DOM. First,
71 increasing delivery of colored and aromatic terrestrial DOM can lead to an increase in CO₂

72 emissions supposing that this terrestrial material gets respired by bacterial communities
73 (Fasching et al., 2014; Lapierre et al., 2013). Second, increase in the export of low molecular
74 weight DOM, either derived from terrestrial sources or produced in-stream, can result in more
75 DOM respired and emitted as CO₂ into the atmosphere (Bodmer et al., 2016; Borges et al.,
76 2018). However, if changes in DOM composition result from an enhancement in aquatic
77 primary production, enhanced respiration of autochthonously-produced DOM shall not lead to
78 higher net CO₂ emissions since the amount of C emitted into the atmosphere would be lower
79 or equivalent to the amount of CO₂ previously fixed by primary aquatic producers. An
80 alternative scenario would be that the release of simple and labile organic compounds derived
81 from autochthonous sources enhances the degradation of terrestrial aromatic DOM by the so-
82 called priming effect (Bianchi, 2011), inducing a final net increase of C emitted to the
83 atmosphere. The priming effect is a process through which labile pool of DOM can enhance
84 (“prime”) the degradation of a more recalcitrant DOM pool based on interactions between
85 microbial communities and/or changes in their functions (Guenet et al., 2010; Kuzyakov et al.,
86 2000) but its occurrence in aquatic ecosystems is highly debated (Attermeyer et al., 2014;
87 Bengtsson et al., 2018; Lambert and Perga, 2019). To determine how human activities may
88 impact the mineralization of terrestrial DOM and infer the consequence on the active role of
89 inland waters into the global C cycle, it is therefore necessary to evaluate the consequences
90 on DOM sources, composition, but also DOM bioavailability and to identify which fraction of
91 the DOM pool fuels respiration. This information is critical to establish the role of human land
92 uses on the linkage between terrestrial and aquatic ecosystems.

93 In this study, we aimed to investigate the impact of human land uses on the role of
94 inland waters as bioreactors with regard to the processing of terrestrial DOM. Water samples
95 were collected twice during the wet season in ten independent catchments selected along a
96 gradient of human pressure (agriculture and urbanization) in the Lake Geneva Basin. Patterns
97 in DOM degradation were investigated based on standardized dark degradation experiments
98 and by the consumption of specific compounds of low molecular weights. Decreases in
99 dissolved organic carbon (DOC) concentrations and changes in DOM composition (assessed
100 by fluorescence spectroscopy) during incubations were used to unravel the contribution of
101 different fractions to the bulk DOM kinetic degradation as well as to the bacterial respiration
102 measured under field conditions. With this approach combining field work and laboratory
103 experiments, we specifically aimed to identify the origin of DOM contributing to bacterial
104 respiration in human-impacted streams and to evaluate the impact of human activities on the
105 biodegradation of terrestrial DOM in Alpine fluvial networks.

106 **2. Material and methods**

107 *2.1 Study sites and sampling*

108 Stream and river waters were collected in ten independent tributaries of Lake
109 Geneva, the largest lake of Western Europe located at the border between France and
110 Switzerland in the Western Alps (Figure 1). Lake Geneva lies in the Alpine foreland between
111 the Alps and the Jura mountains and was carved during Quaternary glaciations mostly into the
112 Tertiary Molasse. Drainage areas of streams and rivers ranged from 11 to 5240 km², Strahler
113 order from 2 to 7, mean elevation from 614 to 2124 m, and land cover was dominated by
114 forests (39±19%), croplands (30±22%), grasslands (13±14%), and urban areas (11±14%)
115 according to the Swiss Federal Office for the Environment (FOEN). Agriculture is dominated
116 by non-irrigated arable lands and vineyards, and forests by coniferous and broad-leaved trees.
117 Selected streams and rivers drained a mosaic of land cover categories and were classified as
118 agro-urban or forest-grassland streams if the sum of croplands and urban areas extents was
119 higher or lower than 50%, respectively (Table 1).

120 Samples were collected on two occasions, at the end of autumn between the 13th and
121 14th of November 2018 and at the end of winter between the 5th and 7th of March 2019.
122 Campaigns were thus carried out during the wet season, i.e., when high discharge conditions
123 may favor greater export of terrestrial DOM (Lambert et al., 2013). The only exception was the
124 Rhône River, that experiences higher water discharge in summer due to the glacio-nival
125 regime of the river (Loizeau and Dominik, 2000). Water temperatures during field campaigns
126 were 10.1±1.8 °C and 6.6±1.1 °C, respectively, but discharge and precipitation conditions at
127 the time of collection were similar (FOEN data). Water was collected below surface in 2 L acid-
128 washed high-density polyethylene (HDPE) bottles and filtered on site. A known volume of
129 water (between 1000 and 1500 mL) was filtered on pre-combusted (450°C for 4 h) Whatman
130 glass fiber filters (GF/F grade, 0.7 µm nominal pore size, 47 mm diameter) for chlorophyll a
131 (Chla) measurements. This filtered water was either stored in 1L acid-washed HDPE bottles
132 for further use in the incubation experiments and the measurements of bacterial metabolism,
133 as described below, or further filtered at 0.2 µm with polyethersulfone (PES) syringe
134 encapsulated filters for dissolved organic carbon (DOC), colored and fluorescent DOM (CDOM
135 and FDOM), soluble reactive phosphorus (SRP), and dissolved inorganic nitrogen (DIN)
136 measurements. Syringe encapsulated filters were first rinsed with ultrapure water (60 mL) in
137 the laboratory and then with 15-20 mL of water from the sampling site before collecting
138 samples. Samples for DOC concentrations were stored in 40 mL acid-washed glass vials with
139 polytetrafluoroethylene (PTFE)-coated septa, and samples for CDOM and FDOM were stored
140 in 40 mL acid-washed amber glass vials with PTFE-coated septa. Samples for SRP, and DIN
141 were stored separately in 50 mL sterile centrifuge tubes. All samples and filters were brought
142 back to the laboratory within 3 hours in cool and dark conditions. Samples for SRP and Chla
143 measurements were frozen at -21°C until analysis. Other samples were stored in a dark
144 chamber at 4-5°C until analysis typically done within the following two weeks.

145 2.2 Characterization of DOM degradation kinetics

146 Incubations were prepared once back to the laboratory. Water samples previously
147 filtered on site at 0.7 μm were divided into 250 mL acid-washed glass flasks and incubated for
148 28 days in the dark at 20°C. A fixed temperature was chosen in order to be able to compare
149 DOM degradation dynamics across our sampling sites at different periods. Because biological
150 activity is strongly impacted by temperature, using water temperature on the field for
151 incubations may have masked patterns in degradation related to differences in the source and
152 composition of DOM (del Giorgio and Davis, 2003). Using a fixed temperature allowed us to
153 investigate how DOM bacterial degradation varied among streams, once the effect of
154 temperature was removed. BDOC, BR, and the bacterial consumption of low molecular weight
155 compounds were incubated in similar conditions (see below), ensuring comparability between
156 water quality, bacterial metabolism, and DOM degradation dynamics. However, consumption
157 and respiration rates should not be considered as representative of field conditions, as
158 incubation temperature – and thus bacterial activity – was higher compared to field conditions.

159 Different subsets of flasks (in triplicates) were prepared and sacrificed for DOC
160 measurements and DOM characterization every 3-5 days for the first 10 days and then every
161 5-8 days up to day 28. Samples were filtered at 0.2 μm with PES syringe encapsulated filters
162 as described above and stored in a dark chamber at 4-5°C. DOC measurements were done
163 within 48h after collection, and CDOM and FDOM analyses over the following week. Dissolved
164 oxygen depletion during the incubations was avoided by leaving a large headspace within the
165 glass flasks and by a regular (every 3-4 days) renewal of the headspace.

166 Several models can be used to characterize DOM degradation kinetic. Here we applied
167 a first-order exponential decay model in order to derive a decay constant describing the overall
168 dynamic of DOM degradation (Lambert and Perga, 2019; Lu et al., 2013; Shang et al., 2018)
169 as well as the size of the short- and a long-term reactive carbon pools (STRC and LTRC,
170 respectively). Decreasing DOC concentrations during the incubations were modeled using
171 GraphPad Prism 8 software according to the following equation:

$$172 \quad \text{DOC}_t = \text{DOC}_{\text{cons}} \cdot e^{-k \cdot t} + \text{DOC}_{\text{residual}}$$

173 where DOC_t (in mg L^{-1}) is the DOC concentration measured at the incubation time t (in
174 days), DOC_{cons} (in mg L^{-1}) the amount of DOC consumed at the end of the incubation, k the
175 decay constant (mgC d^{-1}), and $\text{DOC}_{\text{residual}}$ (in mg L^{-1}) the concentration of the residual pool
176 remaining in solution at the end of the incubation. Biodegradable DOC (BDOC) was calculated
177 as the difference in DOC between the initial and final time. Furthermore, we used the k decay
178 constant from the model to quantify the STRC and LTRC pools: STRC was defined as the
179 amount of DOC consumed within the first six days of incubation and the LTRC as the amount
180 of DOC degraded between days 6 and 28 (Supplementary Figure S1). The separation between

181 STRC and LTRC pools was based on a breakpoint in the degradation curves observed around
182 the 6th day of incubation in almost all experiments. Finally, changes in DOM composition during
183 the incubations were also monitored by fluorescence measurement coupled to parallel factor
184 analysis (PARAFAC) as described below.

185 *2.3 Degradation of low molecular weight compounds*

186 We also determined the consumption of low molecular weight compounds including
187 carbohydrates (CAR), carboxylic and acetic acids (C&AA), and amino acids (AA) using Biolog
188 Ecoplates[®] (Garland and Mills, 1991; Weber and Legge, 2009, 2010). Ecoplates[®] are 96-
189 well microplates containing 31 different carbon substrates (in triplicates) plus a tetrazolium dye.
190 The bacterial respiration activity associated with a specific substrate reduces the tetrazolium
191 dye and produces a color measurable at 590 nm in absorbance. The intensity of color
192 development in color can be related to the amount of substrate consumed (e.g., Berggren and
193 del Giorgio 2015). Water from each site (125 µL) filtered at 0.7 µm was added to each well of
194 one Ecoplates[®] per site, which was then incubated in the dark at 20°C for 3 to 9 days until
195 the average well color development (AWCD) reached an asymptote. The absorbance at 590
196 nm was measured with a TECAN microplate reader one to two times per day. Color
197 development of each carbon substrate was calculated as the blank-corrected absorbance at
198 the time when the AWCD was closest to 0.5 (0.51 ± 0.11 , $n = 60$) following recommendations
199 of Weber and Legge (2010). Carbon substrates were then classified as CAR, C&AA, or AA
200 according to Weber and Legge (2009). The color development for each of these categories
201 was calculated as the mean of the color of the respective substrates normalized by the AWCD.
202 While Ecoplates[®] also include other organic compounds such as polymers or amines/amides,
203 we focused in this study on the consumption of low molecular weight compounds known to
204 support bacterial respiration (Kaplan and Bott, 1989).

205 *2.4 Bacterial respiration measurements*

206 The 0.7 µm-filtered waters used for incubation experiments were also used to measure
207 bacterial respiration (BR) in stream and river waters. BR was determined from the decrease in
208 dissolved oxygen (DO) in 60 mL borosilicate serum bottles filled with water, sealed with a butyl
209 stopper and crimped with an aluminum cap without headspace (3 serum bottles per site).
210 These vials were equipped with SP-PSt7 oxygen planar sensor spots (PreSens) in order to
211 follow DO consumption after 24h of incubation in the dark at 20°C. Initial (1h after the start of
212 incubation) and final DO was recorded using a PreSens Fibox 4 equipped with a fiber-optic
213 oxygen transmitter. Calibration of the PreSens Fibox 4 (two-point calibration at 0 and 100%
214 oxygen saturation) was performed and verified before measurements. BR data were converted
215 into carbon units using a respiratory quotient of 1.

216 2.5 Analytical methods

217 DIN (defined as the sum of nitrate, ammonium and nitrite) was measured by ion
218 chromatography (Metrohm instrument). SRP was determined by spectrophotometry using the
219 ammonium molybdate-potassium antimonyl tartrate method (AFNOR, 2005). DOC
220 concentrations were measured with a total organic carbon analyzer (TOC-L Series,
221 Shimadzu), with a detection limit of 0.01 mg L⁻¹ and a precision better than ±5% based on
222 duplicates and standards. Chla concentrations were determined by spectrophotometry after
223 ethanol extraction (90%). Frozen filters were put in 15 mL sterile centrifuge tubes in which 10
224 mL of ethanol (90%) were added. Tubes were vigorously shaken and then installed in an
225 ultrasonic bath at 70°C for 10 min. Tubes were then stored in a dark chamber for a night,
226 centrifuged 5 min at 4000 rpm and then 10 min at 4000 rpm. Chla concentrations were
227 determined from absorbance at 665 nm after correction of sample turbidity concomitantly
228 measured at 750 nm. Absorbance for CDOM was measured with a Lambda 365 UV/vis
229 spectrophotometer (Perkin Elmer) from 200 to 700 nm (1 nm increment) using a 10 cm quartz
230 cuvette. Napierian absorption coefficients were calculated according to

231
$$a_{\lambda} = 2.303 \cdot \frac{A_{\lambda}}{L}$$

232 where a_{λ} is the absorption coefficient (m⁻¹) at wavelength λ , A_{λ} the absorbance at wavelength
233 λ and L the path length of the optical cell in m. Spectral slopes for the intervals 275–295 and
234 350–400 nm were determined from the linear regression of the *log*-transformed a_{λ} spectra
235 versus wavelength and used to determine the slope ratio (S_R). The slope ratio S_R , calculated
236 as the ratio of $S_{275-295}$ to $S_{350-400}$, is inversely related to the molecular weight distribution of
237 DOM (Helms et al., 2008).

238 FDOM was measured with a Fluorolog-3 spectrofluorometer (Horiba) using a 1 cm
239 quartz cuvette across excitation wavelengths of 270 – 450 nm (5 nm increment) and emission
240 wavelengths of 300 – 500 nm (2 nm increment) in order to build excitation-emission matrices
241 (EEMs). Lamp intensity and instrument calibration were systematically verified before running
242 samples. EEMs were acquired in sample emission to lamp reference mode, and a correction
243 matrix provided by the manufacturer in both excitation and emission dimensions was
244 automatically applied during acquisition. EEMs were then decomposed into individual
245 components using PARAFAC algorithms (Stedmon et al., 2003). Additional samples collected
246 in Lake Geneva and in the Rhône Basin upstream of Lake Geneva were included in the model
247 (total numbers of EEMs > 800). EEMs preprocessing (Raman scattering removal and
248 standardization to Raman units) was performed prior to the PARAFAC modeling.
249 Normalization was done using a Milli-Q water sample run the same day as the sample. An
250 eight components PARAFAC model was obtained using the drEEM 0.3.0 Toolbox (Murphy et
251 al., 2013) for MATLAB (MathWorks, Natick, MA, USA). Split-half analysis, random initialization

252 and visualization of residuals EEMs were used to test and validate the model. The positions of
253 maximums peaks of the PARAFAC components were compared to previous studies with the
254 open fluorescence database OpenFluor using the OpenFluor add-on for the open-source
255 chromatography software OpenChrom (Murphy et al., 2014). The maximum fluorescence F_{Max}
256 values of each component for a particular sample provided by the model were summed to
257 calculate the total fluorescence signal F_{Tot} of the sample in Raman units. The relative
258 abundance of any particular PARAFAC component X was then calculated as
259 $\%C_X = F_{Max}(X)/F_{Tot}$. Precision of EEMs-PARAFAC, based on replicate measurements ($n = 5$) of
260 different samples, was ± 0.001 R.U. for F_{Max} values of components C1 to C5 and ± 0.003 R.U
261 for F_{Max} values of components C6 to C8, and $\pm 0.2\%$ for $\%C_X$ for components C1 to C5 and
262 $\pm 0.5\%$ for components C6 to C8. Finally, the variations of PARAFAC components during
263 incubations were expressed as $(F_{Max}(X)_{tf} - F_{Ma}(X)_{t0})/F_{Max}(X)_{t0}$ with t_0 and t_f the initial and final
264 values of F_{Max} , respectively. Based on the accuracy of EEM-PARAFAC measurements
265 estimated by replicate measurements (see above), we considered variations to be significant
266 if the median of response ratio was higher than ± 0.05 for components C1 to C5 and ± 0.1 for
267 components C6 to C8.

268 2.6 Statistical analyses

269 Differences in water quality, DOM degradability, BR and consumption of low molecular
270 weight compounds between agro-urban and forest-grassland streams were tested with a Mann
271 Whitney unpaired t -test at 0.05 confidence interval level. Differences between the sampling
272 periods were investigated by paired t -tests. The level of significance was set to 0.05. The
273 ROUT method implemented in the GraphPad Prism 8 software was used to identify potential
274 outliers. A principal component analysis (PCA) was performed to investigate the importance
275 of human land uses on water quality relative to other geomorphological features (e.g. mean
276 elevation) of the study sites. The data selected for the PCA were DOC, SRP, DIN, and the
277 relative abundance of PARAFAC components collected during the two main campaigns. The
278 PCA was done using the *prcomp* function in the R software, and the *factoextra* package was
279 used to identify the variables that contribute the most to the first two dimensions of the PCA.
280 The sum of cropland and urban areas extents were used as descriptive variables in the PCA
281 biplot.

282 3. Results

283 3.1 Water quality and DOM composition across catchments

284 Hydro-climatic conditions were similar for the two sampling campaigns that occurred
285 during high winter base flow level and no significant difference was found in the overall water
286 quality between the two campaigns (not shown). However, significant differences were

287 observed between sampling sites depending on the dominant land cover (Figures 2 and 3).
288 Chla (total range of variation between sites and periods from 0.2 to 54.9 $\mu\text{g L}^{-1}$), SRP (from 0.5
289 to 34.5 $\mu\text{g L}^{-1}$), DIN (from 0.3 to 8.8 mg L^{-1}), and DOC (from 0.7 to 5.9 mg L^{-1}) concentrations
290 were higher in agro-urban streams that were also characterized by DOM of lower molecular
291 weight (higher S_R values) and higher BR values (Figure 2).

292 Eight PARAFAC components were identified in our study sites (Table 2, Supplementary
293 Figure S2), all of which having been already described in previous studies (Graeber et al.,
294 2012; Lambert et al., 2017; Massicotte and Frenette, 2011; Stedmon et al., 2011; Stedmon
295 and Markager, 2005; Williams et al., 2016; Yamashita et al., 2010). Components included three
296 humic-like fluorophores (C1, C3, C4), one fulvic-like fluorophore (C2), two microbial protein-
297 like fluorophores (C5 and C6), and the common tryptophane (C7) and tyrosine (C8) protein-
298 like fluorophores. All components exhibited higher F_{Max} values in agro-urban streams, although
299 the most notable increases were observed for protein-like fluorophores (Figure 3).

300 The two first components of the PCA explained 72.4% of the variance (Figure 4). The
301 first principal component (PC1) was related to protein-like components C6 to C8, DOC and
302 SRP (positive scores) and to humic-like components C2 to C4 (negative scores), whereas the
303 second principal component (PC2) was related to higher C5, DOC and DIN concentrations
304 (positive scores) and lower C1 (negative score). The results of the PCA showed that the
305 variability in DOM composition and nutrient loadings was largely driven by land uses (Figure
306 4). Scores along PC1 were positively related to croplands (Pearson $r = 0.49$, $p = 0.0265$), urban
307 areas (Pearson $r = 0.63$, $p = 0.0027$) and negatively to forest (Pearson $r = -0.72$, $p = 0.0003$)
308 and grasslands (Pearson $r = -0.48$, $p = 0.0295$), but not to catchment area (Pearson $r = -0.04$,
309 $p = 0.86$), Strahler order (Pearson $r = 0.13$, $p = 0.57$) or mean elevation (Pearson $r = -0.32$, p
310 $= 0.18$). No relationship was found between PC2 and geomorphological properties of sampling
311 sites, suggesting an in-stream origin for the components C1 and C5. Based on the optical
312 properties of PARAFAC components (Table 2), PC1 represented a shift in the dominant
313 composition of DOM from terrestrial (components C2-C4) to autochthonous (C6-C8)
314 signatures as human disturbance (croplands + urban areas) increases. PC2, however,
315 reflected the in-stream generation of DOM through photodegradation (C1) and bacterial
316 processing of DOM (C5).

317 *3.2 Kinetics of bacterial DOM degradation and consumption of low molecular weight* 318 *compounds*

319 All incubations were successfully modeled by a first order exponential decay model (r^2
320 $= 0.98 \pm 0.02$), and we estimated the decay constants and the amounts of BDOC, STRC and
321 LTRC pools for all experiments (Figure 5). BDOC ranged from 0.2 to 2.3 mg L^{-1} (mean =
322 $1.0 \pm 0.6 \text{ mg L}^{-1}$), corresponding to 9.7 to 57.6% of initial DOC (mean = $33.8 \pm 11\%$). Higher

323 amount of BDOC in agro-urban streams was accompanied by higher decay constants (from
324 0.01 to 0.26 d⁻¹, mean = 0.12±0.07 d⁻¹) and greater availability of STRC (from 0.01 to 1.3 mg
325 L⁻¹, mean = 0.5±0.4 mg L⁻¹) but no significant difference was observed regarding the amount
326 of LTRC (from 0.1 to 1.0 mg L⁻¹, mean = 0.5±0.3 mg L⁻¹) across stream categories. Both the
327 STRC and LTRC pools were positively correlated with DOC concentrations (Pearson r = 0.79,
328 p < 0.0001 and Pearson r = 0.68, p = 0.0013, respectively), leading to a positive but weak
329 relationship between the STRC and LTRC pools (Person r = 0.49, p = 0.03). STRC was
330 correlated to all components when expressed in F_{Max} values, but only with protein-like
331 components when expressed as a relative contribution to the total fluorescence signal,
332 suggesting an autochthonous origin for this reactive C. On the contrary, the LTRC related to
333 FMax values of C1-C4 components but not with the protein-like components, suggesting that
334 this reactive C originated from terrestrial sources. The total amount of BDOC, decay constants
335 and the size of STRC were significantly related to the C6-C8 protein-like components (Figure
336 6). There was however no relationship between the decay constant k and LTRC.

337 The S_R values decreased in all experiments (Supplementary Figure S3), indicating an
338 increase in the average molecular weight of DOM during incubations as low molecular weight
339 compounds were preferentially degraded. Regarding the evolution of the different fractions of
340 DOM during incubations, no significant changes in F_{Max} values were observed for humic-like
341 components during incubations (Figure 7). Component C5, however, tended to be produced
342 upon bacterial activity. On the contrary, the other protein-like components C6 – C8 were
343 consumed during incubations. Finally, the consumption of low molecular weights compounds
344 was greater in agro-urban streams for AA and CAR molecules, but no difference was observed
345 regarding the degradation of C&AA (Figure 8).

346 4. Discussion

347 The bacterial degradation of DOM along fluvial networks contributes to CO₂ emissions
348 toward the atmosphere (Lapierre et al., 2013). Human activities are expected to alter the role
349 of inland waters in the global carbon cycle by disturbing DOM sources and composition
350 (Xenopoulos et al., 2021). Keeping in mind that our study focused mainly on small size
351 catchments during the wet period, our results highlighted that the enhanced production and
352 accumulation of autochthonous DOM in human-disturbed streams was quickly cycled back to
353 the atmosphere by heterotrophic bacteria. From a greenhouse gas emission perspective, the
354 respiration of this highly reactive DOM pool may have a limited impact on C budgets in human-
355 disturbed catchments.

356 4.1 Origin and biodegradability of DOM in agro-urban streams

357 DOM in human-disturbed streams was characterized by a lower average molecular
358 weight compared to forest-grassland streams reflecting the influence of human activities on
359 DOM sources and composition in the Lake Geneva Basin. The increase in protein-like DOM
360 due to a greater autochthonous productivity is a recurrent observation across aquatic
361 ecosystems draining agricultural and urban landscapes (Stanley et al., 2012; Xenopoulos et
362 al., 2021). Enrichment in nutrients and increased light exposure in agriculture and urban
363 streams can promote primary production (Catford et al., 2007; Taylor et al., 2004), and greater
364 algal biomass in our study sites was evidenced by higher Chl_a concentrations (Figure 2) and
365 the subsequent release of protein-like components (C6 – C8) related to algal DOM (Figure 3,
366 Table 2). Although C5 also relates to autochthonous biological production (Stedmon et al.,
367 2011), its accumulation during incubation experiments implies that this component reflected
368 DOM recently produced by bacterial activity (Figure 7). Higher F_{Max} values of C5 in human-
369 impacted catchments thus represented a positive feedback loop where greater primary
370 production enhanced bacterial activity that shaped DOM composition toward a more bacterial
371 signature (Harfmann et al., 2019; Williams et al., 2010). Although of lower amplitude, higher
372 F_{Max} values of components associated with terrestrial inputs (C2 – C4, Table 2) and/or
373 photobleaching (C1) indicated a more efficient export of terrestrial material in agro-urban
374 streams. As urbanization tends to limit the hydrological connection between terrestrial and
375 aquatic ecosystems (e.g. Hosen et al. 2014), it is likely that this pattern reflected greater
376 erosion of agricultural soils (Celik, 2005; Graeber et al., 2012).

377 Along with changes in DOM sources and composition, the bioavailability of DOM was
378 strongly impacted by croplands and urbanization (Figure 5). The positive effect of human land
379 use on the total amount and decay constants of bioavailable DOM agrees with previous studies
380 (Hosen et al., 2014; Parr et al., 2015), but our results further link this effect to the generation
381 of a highly reactive pool of organic molecules derived from in stream primary production. Algae
382 are known to be a major source of low molecular weight compounds in aquatic ecosystems
383 through exudation and cell lysis (Kaplan and Bott, 1989) which are rapidly taken up by
384 heterotrophic bacteria (Descy, 2002). A higher consumption of amino acids and carbohydrates
385 concomitant with higher Chl_a concentrations in agro-urban streams agrees with the generation
386 of labile molecules derived from primary production. The loss of protein-like components
387 paralleled by an increase in the average molecular weight during incubations also evidences
388 the efficient degradation of this DOM from algal origin. Moreover, the strong relationships
389 between the amount of BDOC, the decay constants k , and the size of the STRC pool with the
390 initial contribution of protein-like components C6-C8 (Figure 6) provide another evidence that
391 greater DOM bioavailability in agro-urban streams resulted from greater in-stream production.

392 Contrary to STRC, the LTRC pools were similar across agro-urban and forest-
393 grassland streams. In line with a recent study carried out in Swedish inland waters (Soares et
394 al., 2019), the STRC and LTRC pools were comparable in size but no evidence of interaction
395 was observed between the bioavailability of DOM on short and long timescales. The positive
396 but weak relationship between STRC and LTRC likely reflected a greater amount of
397 bioavailable DOM as human disturbance increased, as the latter enhanced both primary
398 production and terrestrial export. Moreover, each pool related to specific DOM fractions.
399 Similar observations were reported in Swedish rivers (Soares et al., 2019), in southern Québec
400 (Guillemette and del Giorgio, 2011), or also in the Hudson River (del Giorgio and Pace, 2008).
401 Overall, our findings are in good agreement with the idea that STRC is sustained by algal
402 growth, whereas the consumption of DOC at longer timescales is rather related to terrestrial
403 inputs of DOM (e.g., Guillemette and del Giorgio, 2011).

404 The humic-like components showed no significant variations during incubations (Figure
405 7) despite the ability of bacterial communities to degrade complex aromatic molecules (Catalán
406 et al., 2017; Fasching et al., 2014; Logue et al., 2016). While the stability of the C1 component
407 during bioassays is consistent with the fact that photoproducts may be resistant to
408 further bacterial degradation (Tranvik et al., 2001), the lack of variation of C2-C4 components
409 may reflect an equilibrium between the bacterial consumption and production of molecules
410 contributing to the humic-like signatures. Experimental and field studies have shown that
411 heterotrophic bacterial communities are able to produce molecules fluorescing in the region of
412 EEMs commonly attributed to humic-like material from terrestrial origin (Amaral et al., 2016;
413 Fox et al., 2017; Guillemette and del Giorgio, 2012). It is therefore possible that the alteration
414 of terrestrial DOM upon bacterial activity may not have been captured by optical
415 measurements. Addressing this point would require the characterization of DOM at the
416 molecular level (e.g., Kim et al., 2006).

417 *4.2 Linking bacterial respiration to DOM origin and implication of human activities on the role* 418 *of inland water in the C cycle*

419 The positive influence of enhanced primary production on the absolute amount of
420 biodegradable DOM in human-disturbed streams agrees with previous studies (Hosen et al.,
421 2014; Parr et al., 2015), but our results suggest that the impact regarding the role of inland
422 waters in the context of the C cycle may be limited. Higher BR in agro-urban streams was
423 indeed mostly related to the accumulation and mineralization of molecules generated by
424 aquatic primary producers (Figure 9A), although the photodegradation of terrestrial DOM could
425 also fuel BR through the transformation of complex and aromatic molecules into compounds
426 of lower molecular weight (Bertilsson and Tranvik, 1998) as suggested by the positive
427 relationship between BR and C1 (Figure 9B). Therefore, our results point to a limited effect of

428 STRC on greenhouse gas emission as most of the C released toward the atmosphere upon
429 bacterial respiration corresponded to atmospheric CO₂ previously fixed by aquatic producers
430 and converted into biomass.

431 We observed, however, an influence of human activities on the transformation of DOM
432 along fluvial networks. Despite the large range of size of our sampling sites (Table 1), we found
433 no relationship between Strahler order (ranging from 2 to 7) and DOM composition and
434 reactivity. This observation contrasts with a recent study where stream order (ranging from 1
435 to 4) correlated negatively with humic-like DOM but positively with protein-like DOM (Shang et
436 al., 2018), a pattern consistent with a general conceptual trend describing DOM
437 transformations along the fluvial continuum. Indeed, the control of DOM dynamic along the
438 river continuum is expected to shift from a dominant influence of terrestrial inputs in the
439 headwaters to a dominant influence of in-stream removal and autochthonous production as
440 stream order increases (Creed et al. 2015). In our study, however, human land uses had a
441 major role in controlling DOM sources and reactivity at the basin scale (Figure 4). The only
442 exception was a positive correlation between Strahler order and the relative proportion of C5
443 (Supplementary Figure S4), indicating that the degradation of autochthonous DOM in agro-
444 urban streams led to a bacterial imprint on the DOM pool that persists along the aquatic
445 continuum (Harfmann et al., 2019; Williams et al., 2010).

446 **5. Conclusion**

447 In this study, human land uses were found to alter the terrestrial and aquatic sources
448 of freshwater DOM in an Alpine fluvial network. Enhanced primary production in human-
449 disturbed catchments led to the accumulation of highly reactive molecules of low molecular
450 weight which in turn stimulated bacterial respiration. Despite a dominant influence on DOM
451 composition and reactivity at the basin scale, our study suggests that human land uses may
452 have a limited effect in terms of net C flux exchanges between inland waters and atmosphere
453 related to DOM mineralization by heterotrophic bacterial communities. However, further
454 studies should perform incubation and respiration measurements at *in situ* conditions to
455 improve our understanding of different bioreactive DOC pools to better constrain C budgets.

456 Considering that an enrichment in protein-like DOM due to greater autochthonous
457 production is a recurrent observation in agricultural and urban catchments (Stanley et al., 2012;
458 Xenopoulos et al., 2021), our results are likely not limited to the Lake Geneva Basin. However,
459 seasonal and longitudinal variations in DOM sources and composition should be considered
460 along with the fact that the net effects of agriculture and urbanization on freshwater DOM vary
461 widely depending on the environmental context (Stanley et al., 2012). While our results are in
462 line with previous works (Hosen et al., 2014; Parr et al., 2015), they contrast with studies

463 reporting no influence of human land uses on the bacterial consumption of DOM (Kadjeski et
464 al., 2020; Lu et al., 2013) or higher DOM degradability in agricultural streams (Shang et al.,
465 2018). Therefore, additional works on the links between human activities and DOM reactivity
466 and fate are needed in order to fully assess the future of inland waters in the context of the
467 global C cycle.

468 **Data availability** Data used in the manuscript are available in the supplementary information
469 (Table S1 and S2).

470 **Author Contributions:** T. L. conceived the study with contribution from M.-E. P. T. L., P. P.,
471 and N. E. collected field samples. T. L. made laboratory analysis. T.L. drafted the
472 manuscript which was substantially commented upon and amended by M.-E. P., P. P., and
473 N. E. All co-authors approved the manuscript.

474 **Competing interests:** The authors declare that they have no conflict of interest.

475 **Acknowledgements:** We thank Laetitia Monbaron and Micaela Faria for assistance in the
476 laboratory and Janine Rüegg for her comments on an initial version of the manuscript. We
477 gratefully acknowledge the anonymous reviewers who provided very constructive and
478 insightful comments on the earlier versions of this manuscript.

479 **Financial Support:** The research was funded by the Swiss National Science Foundation
480 grant number 200021_175530 (project CARBOGEN).

481 **References**

482 AFNOR: NF EN ISO 6878 : Qualité de l'eau Dosage du phosphore - Méthode
483 spectrométrique au molybdate d'ammonium, AFNOR, 2005.

484 Amaral, V., Graeber, D., Calliari, D. and Alonso, C.: Strong linkages between DOM optical
485 properties and main clades of aquatic bacteria, *Limnol. Oceanogr.*, 61(3), 906–918,
486 doi:10.1002/lno.10258, 2016.

487 Attermeyer, K., Hornick, T., Kayler, Z. E., Bahr, A., Zwirnmann, E., Grossart, H. P. and
488 Premke, K.: Enhanced bacterial decomposition with increasing addition of autochthonous to
489 allochthonous carbon without any effect on bacterial community composition,
490 *Biogeosciences*, 11(6), 1479–1489, doi:10.5194/bg-11-1479-2014, 2014.

491 Bengtsson, M. M., Attermeyer, K. and Catalán, N.: Interactive effects on organic matter
492 processing from soils to the ocean: are priming effects relevant in aquatic ecosystems?,
493 *Hydrobiologia*, 822(1), doi:10.1007/s10750-018-3672-2, 2018.

494 Berggren, M. and del Giorgio, P. A.: Distinct patterns of microbial metabolism associated to
495 riverine dissolved organic carbon of different source and quality, *J. Geophys. Res. G*
496 *Biogeosciences*, 120, 989–999, doi:10.1002/2015JG002963, 2015.

497 Berggren, M., Laudon, H., Haei, M., Ström, L. and Jansson, M.: Efficient aquatic bacterial
498 metabolism of dissolved low-molecular-weight compounds from terrestrial sources, *ISME J.*,
499 4(3), 408–416, doi:10.1038/ismej.2009.120, 2010.

500 Bertilsson, S. and Tranvik, L. J.: Photochemically produced carboxylic acids as substrates for
501 freshwater bacterioplankton, *Limnol. Oceanogr.*, 43(5), 885–895,

502 doi:10.4319/lo.1998.43.5.0885, 1998.

503 Bianchi, T. S.: The role of terrestrially derived organic carbon in the coastal ocean: A
504 changing paradigm and the priming effect, *Proc. Natl. Acad. Sci.*, 108(49), 19473–19481,
505 doi:10.1073/pnas.1017982108, 2011.

506 Bodmer, P., Heinz, M., Pusch, M., Singer, G. and Premke, K.: Carbon dynamics and their
507 link to dissolved organic matter quality across contrasting stream ecosystems, *Sci. Total*
508 *Environ.*, 553, 574–586, doi:10.1016/j.scitotenv.2016.02.095, 2016.

509 Borges, A. V., Darchambeau, F., Lambert, T., Bouillon, S., Morana, C., Brouyère, S.,
510 Hakoun, V., Jurado, A., Tseng, H. C., Descy, J. P. and Roland, F. A. E.: Effects of
511 agricultural land use on fluvial carbon dioxide, methane and nitrous oxide concentrations in a
512 large European river, the Meuse (Belgium), *Sci. Total Environ.*, 610–611(August 2017), 342–
513 355, doi:10.1016/j.scitotenv.2017.08.047, 2018.

514 Catalán, N., Casas-Ruiz, J. P., von Schiller, D., Proia, L., Obrador, B., Zwirnmann, E. and
515 Marcé, R.: Biodegradation kinetics of dissolved organic matter chromatographic fractions, a
516 case study in an intermittent river, *J. Geophys. Res. Biogeosciences*, 122, 131–144,
517 doi:10.1002/2016JG003512, 2017.

518 Catford, J. A., Walsh, C. J. and Beardall, J.: Catchment urbanization increases benthic
519 microalgal biomass in streams under controlled light conditions, *Aquat. Sci.*, 69(4), 511–522,
520 doi:10.1007/s00027-007-0907-0, 2007.

521 Celik, I.: Land-use effects on organic matter and physical properties of soil in a southern
522 Mediterranean highland of Turkey, *Soil Tillage Res.*, 83(2), 270–277,
523 doi:10.1016/j.still.2004.08.001, 2005.

524 Cole, J. J., Prairie, Y. T., Caraco, N. F., McDowell, W. H., Tranvik, L. J., Striegl, R. G.,
525 Duarte, C. M., Kortelainen, P., Downing, J. A., Middelburg, J. J. and Melack, J.: Plumbing the
526 global carbon cycle: Integrating inland waters into the terrestrial carbon budget, *Ecosystems*,
527 10(1), 171–184, doi:10.1007/s10021-006-9013-8, 2007.

528 Creed, I. F., McKnight, D. M., Pellerin, B. A., Green, M. B., Bergamaschi, B. A., Aiken, G. R.,
529 Burns, D. A., Findlay, S. E. G., Shanley, J. B., Striegl, R. G., Aulenbach, B. T., Clow, D. W.,
530 Laudon, H., McGlynn, B. L., McGuire, K. J., Smith, R. A. and Stackpoole, S. M.: The river as
531 a chemostat: fresh perspectives on dissolved organic matter flowing down the river
532 continuum, *Can. J. Fish. Aquat. Sci.*, 72(8), 1272–1285, doi:10.1139/cjfas-2014-0400, 2015.

533 Descy, J.-P.: Phytoplankton production, exudation and bacterial reassimilation in the River
534 Meuse (Belgium), *J. Plankton Res.*, 24(3), 161–166, doi:10.1093/plankt/24.3.161, 2002.

535 Ekblad, A. and Bastviken, D.: Deforestation releases old carbon, *Nat. Geosci.*, 12(July),
536 doi:10.1038/s41561-019-0394-7, 2019.

537 Fasching, C., Behounek, B., Singer, G. A. and Battin, T. J.: Microbial degradation of
538 terrigenous dissolved organic matter and potential consequences for carbon cycling in
539 brown-water streams, *Sci. Rep.*, 4, 1–7, doi:10.1038/srep04981, 2014.

540 Fox, B. G., Thorn, R. M. S., Anesio, A. M. and Reynolds, D. M.: The in situ bacterial
541 production of fluorescent organic matter; an investigation at a species level, *Water Res.*, 125,
542 350–359, doi:10.1016/j.watres.2017.08.040, 2017.

543 Fuß, T., Behounek, B., Ulseth, A. J. and Singer, G. A.: Land use controls stream ecosystem
544 metabolism by shifting dissolved organic matter and nutrient regimes, *Freshw. Biol.*, 62(3),
545 582–599, doi:10.1111/fwb.12887, 2017.

546 Garland, J. L. and Mills, A. L.: Classification and characterization of heterotrophic microbial
547 communities on the basis of patterns of community-level sole-carbon-source utilization, *Appl.*
548 *Environ. Microbiol.*, 57(8), 2351–2359, doi:10.1128/aem.57.8.2351-2359.1991, 1991.

549 Giling, D. P., Grace, M. R., Thomson, J. R., Mac Nally, R. and Thompson, R. M.: Effect of

550 Native Vegetation Loss on Stream Ecosystem Processes: Dissolved Organic Matter
551 Composition and Export in Agricultural Landscapes, *Ecosystems*, 17(1), 82–95,
552 doi:10.1007/s10021-013-9708-6, 2014.

553 del Giorgio, P. A. and Davis, J.: Patterns in DOM lability and consumption across aquatic
554 ecosystems, in *Aquatic ecosystems: Interactivity of dissolved organic matter*, pp. 399–424.,
555 2003.

556 Graeber, D., Gelbrecht, J., Pusch, M. T., Anlanger, C. and von Schiller, D.: Agriculture has
557 changed the amount and composition of dissolved organic matter in Central European
558 headwater streams, *Sci. Total Environ.*, 438, 435–446, doi:10.1016/j.scitotenv.2012.08.087,
559 2012.

560 Guenet, B., Danger, M., Abbadie, L. and Lacroix, G.: Priming effect: bridging the gap
561 between terrestrial and aquatic ecology, *Ecology*, 91(10), 2850–2861, doi:10.1890/09-
562 1968.1, 2010.

563 Guillemette, F. and del Giorgio, P. A.: Reconstructing the various facets of dissolved organic
564 carbon bioavailability in freshwater ecosystems, *Limnol. Oceanogr.*, 56(2), 734–748,
565 doi:10.4319/lo.2011.56.2.0734, 2011.

566 Guillemette, F. and del Giorgio, P. A.: Simultaneous consumption and production of
567 fluorescent dissolved organic matter by lake bacterioplankton, *Environ. Microbiol.*, 14(6),
568 1432–1443, doi:10.1111/j.1462-2920.2012.02728.x, 2012.

569 Harfmann, J. L., Guillemette, F., Kaiser, K., Spencer, R. G. M., Chuang, C. Y. and Hernes, P.
570 J.: Convergence of Terrestrial Dissolved Organic Matter Composition and the Role of
571 Microbial Buffering in Aquatic Ecosystems, *J. Geophys. Res. Biogeosciences*, 124(10),
572 3125–3142, doi:10.1029/2018JG004997, 2019.

573 Helms, J. R., Stubbins, A., Ritchie, J. D., Minor, E. C., Kieber, D. J. and Mopper, K.:
574 Absorption Spectral Slopes and Slope Ratios As Indicators of Molecular Weight, Source, and
575 Photobleaching of Chromophoric Dissolved Organic Matter, , 53(3), 955–969, 2008.

576 Hosen, J. D., McDonough, O. T., Febria, C. M. and Palmer, M. A.: Dissolved organic matter
577 quality and bioavailability changes across an urbanization gradient in headwater streams,
578 *Environ. Sci. Technol.*, 48(14), 7817–7824, doi:10.1021/es501422z, 2014.

579 Hu, Y., Lu, Y. H., Edmonds, J. W., Liu, C., Wang, S., Das, O., Liu, J. and Zheng, C.:
580 Hydrological and land use control of watershed exports of dissolved organic matter in a large
581 arid river basin in northwestern China, *J. Geophys. Res. Biogeosciences*, 121(2), 466–478,
582 doi:10.1002/2015JG003082, 2016.

583 Humbert, G., Parr, T. B., Jeanneau, L., Dupas, R., Petitjean, P., Akkal-Corfini, N., Viaud, V.,
584 Pierson-Wickmann, A. C., Denis, M., Inamdar, S., Gruau, G., Durand, P. and Jaffrézic, A.:
585 Agricultural Practices and Hydrologic Conditions Shape the Temporal Pattern of Soil and
586 Stream Water Dissolved Organic Matter, *Ecosystems*, 23(7), 1325–1343,
587 doi:10.1007/s10021-019-00471-w, 2020.

588 Kadjeski, M., Fasching, C. and Xenopoulos, M. A.: Synchronous Biodegradability and
589 Production of Dissolved Organic Matter in Two Streams of Varying Land Use, *Front.*
590 *Microbiol.*, 11(November), 1–14, doi:10.3389/fmicb.2020.568629, 2020.

591 Kaplan, L. A. and Bott, T. L.: Diel fluctuations in bacterial activity on streambed substrata
592 during vernal algal blooms: Effects of temperature, water chemistry, and habitat, *Limnol.*
593 *Oceanogr.*, 34(4), 718–733, doi:10.4319/lo.1989.34.4.0718, 1989.

594 Kim, S., Kaplan, L. A. and Hatcher, P. G.: Biodegradable dissolved organic matter in a
595 temperate and a tropical stream determined from ultra – high resolution mass spectrometry, ,
596 51(2), 1054–1063, 2006.

597 Kuzyakov, Y., Friedel, J. K. and Stahr, K.: Review of mechanisms and quantification of

598 priming effects, *Soil Biol. Biochem.*, 32(11–12), 1485–1498, doi:10.1016/S0038-
599 0717(00)00084-5, 2000.

600 Lambert, T. and Perga, M.-E.: Non-conservative patterns of dissolved organic matter
601 degradation when and where lake water mixes, *Aquat. Sci.*, 81(4), 64, doi:10.1007/s00027-
602 019-0662-z, 2019.

603 Lambert, T., Pierson-Wickmann, A. C., Gruau, G., Jaffrezic, A., Petitjean, P., Thibault, J. N.
604 and Jeanneau, L.: Hydrologically driven seasonal changes in the sources and production
605 mechanisms of dissolved organic carbon in a small lowland catchment, *Water Resour. Res.*,
606 49(9), 5792–5803, doi:10.1002/wrcr.20466, 2013.

607 Lambert, T., Bouillon, S., Darchambeau, F., Morana, C., Roland, F. A. E., Descy, J. P. and
608 Borges, A. V.: Effects of human land use on the terrestrial and aquatic sources of fluvial
609 organic matter in a temperate river basin (The Meuse River, Belgium), *Biogeochemistry*,
610 136(2), 191–211, doi:10.1007/s10533-017-0387-9, 2017.

611 Landsman-Gerjoi, M., Perdrial, J. N., Lancellotti, B., Seybold, E., Schroth, A. W., Adair, C.
612 and Wymore, A.: Measuring the influence of environmental conditions on dissolved organic
613 matter biodegradability and optical properties: a combined field and laboratory study,
614 *Biogeochemistry*, 149(1), 37–52, doi:10.1007/s10533-020-00664-9, 2020.

615 Lapierre, J. F., Guillemette, F., Berggren, M. and Del Giorgio, P. A.: Increases in terrestrially
616 derived carbon stimulate organic carbon processing and CO₂ emissions in boreal aquatic
617 ecosystems, *Nat. Commun.*, 4, doi:10.1038/ncomms3972, 2013.

618 Logue, J. B., Stedmon, C. A., Kellerman, A. M., Nielsen, N. J., Andersson, A. F., Laudon, H.,
619 Lindström, E. S. and Kritzberg, E. S.: Experimental insights into the importance of aquatic
620 bacterial community composition to the degradation of dissolved organic matter, *ISME J.*,
621 10(3), 533–545, doi:10.1038/ismej.2015.131, 2016.

622 Loizeau, J. L. and Dominik, J.: Evolution of the upper Rhone river discharge and suspended
623 sediment load during the last 80 years, *Aquat. Sci.*, 62, 54–67, doi:10.1007/s000270050075,
624 2000.

625 Lu, Y., Bauer, J. E., Canuel, E. A., Yamashita, Y., Chambers, R. M. and Jaffé, R.:
626 Photochemical and microbial alteration of dissolved organic matter in temperate headwater
627 streams associated with different land use, *J. Geophys. Res. Biogeosciences*, 118(2), 566–
628 580, doi:10.1002/jgrg.20048, 2013.

629 Lu, Y. H., Bauer, J. E., Canuel, E. A., Chambers, R. M., Yamashita, Y., Jaffé, R. and Barrett,
630 A.: Effects of land use on sources and ages of inorganic and organic carbon in temperate
631 headwater streams, *Biogeochemistry*, 119(1–3), 275–292, doi:10.1007/s10533-014-9965-2,
632 2014.

633 Massicotte, P. and Frenette, J. J.: Spatial connectivity in a large river system: Resolving the
634 sources and fate of dissolved organic matter, *Ecol. Appl.*, 21(7), 2600–2617, doi:10.1890/10-
635 1475.1, 2011.

636 Mayorga, E., Aufdenkampe, A. K., Masiello, C. A., Krusche, A. V., Hedges, J. I., Quay, P. D.,
637 Richey, J. E. and Brown, T. A.: Young organic matter as a source of carbon dioxide
638 outgassing from Amazonian rivers, *Nature*, 436(7050), 538–541, doi:10.1038/nature03880,
639 2005.

640 Murphy, K. R., Stedmon, C. A., Graeber, D. and Bro, R.: Fluorescence spectroscopy and
641 multi-way techniques. PARAFAC, *Anal. Methods*, 5(23), 6557, doi:10.1039/c3ay41160e,
642 2013.

643 Murphy, K. R., Stedmon, C. A., Wenig, P. and Bro, R.: OpenFluor– an online spectral library
644 of auto-fluorescence by organic compounds in the environment, *Anal. Methods*, 6(3), 658–
645 661, doi:10.1039/C3AY41935E, 2014.

646 Parr, T. B., Cronan, C. S., Ohno, T., Findlay, S. E. G., Smith, S. M. C. and Simon, K. S.:
647 Urbanization changes the composition and bioavailability of dissolved organic matter in
648 headwater streams, *Limnol. Oceanogr.*, 60(3), 885–900, doi:10.1002/lno.10060, 2015.

649 Petrone, K. C., Fellman, J. B., Hood, E., Donn, M. J. and Grierson, P. F.: The origin and
650 function of dissolved organic matter in agro-urban coastal streams, *J. Geophys. Res.*
651 *Biogeosciences*, 116(1), doi:10.1029/2010JG001537, 2011.

652 Reche, I., Pace, M. L. and Cole, J. J.: Interactions of photobleaching and inorganic nutrients
653 in determining bacterial growth on colored dissolved organic carbon, *Microb. Ecol.*, 36(3),
654 270–280, doi:10.1007/s002489900114, 1998.

655 Shang, P., Lu, Y. H., Du, Y. X., Jaffé, R., Findlay, R. H. and Wynn, A.: Climatic and
656 watershed controls of dissolved organic matter variation in streams across a gradient of
657 agricultural land use, *Sci. Total Environ.*, 612, 1442–1453,
658 doi:10.1016/j.scitotenv.2017.08.322, 2018.

659 Stanley, E. H., Powers, S. M., Lottig, N. R., Buffam, I. and Crawford, J. T.: Contemporary
660 changes in dissolved organic carbon (DOC) in human-dominated rivers: Is there a role for
661 DOC management?, *Freshw. Biol.*, 57(SUPPL. 1), 26–42, doi:10.1111/j.1365-
662 2427.2011.02613.x, 2012.

663 Stedmon, C. A. and Markager, S.: Resolving the variability in dissolved organic matter
664 fluorescence in a temperate estuary and its catchment using PARAFAC analysis., *Limnol.*
665 *Oceanogr.*, 50(2), 686–697, doi:10.4319/lo.2005.50.2.0686, 2005.

666 Stedmon, C. A., Markager, S. and Bro, R.: Tracing dissolved organic matter in aquatic
667 environments using a new approach to fluorescence spectroscopy, *Mar. Chem.*, 82(3–4),
668 239–254, doi:10.1016/S0304-4203(03)00072-0, 2003.

669 Stedmon, C. A., Thomas, D. N., Papadimitriou, S., Granskog, M. A. and Dieckmann, G. S.:
670 Using fluorescence to characterize dissolved organic matter in Antarctic sea ice brines, *J.*
671 *Geophys. Res. Biogeosciences*, 116(3), 1–9, doi:10.1029/2011JG001716, 2011.

672 Taylor, S. L., Roberts, S. C., Walsh, C. J. and Hatt, B. E.: Catchment urbanisation and
673 increased benthic algal biomass in streams: Linking mechanisms to management, *Freshw.*
674 *Biol.*, 49(6), 835–851, doi:10.1111/j.1365-2427.2004.01225.x, 2004.

675 Tranvik, L., Bertilsson, S. and Letters, E.: Contrasting effects of solar UV radiation on
676 dissolved organic sources for bacterial growth, *Ecol. Lett.*, 4(5), 458–463, doi:10.1046/j.1461-
677 0248.2001.00245.x, 2001.

678 Weber, K. P. and Legge, R. L.: One-dimensional metric for tracking bacterial community
679 divergence using sole carbon source utilization patterns, *J. Microbiol. Methods*, 79(1), 55–61,
680 doi:10.1016/j.mimet.2009.07.020, 2009.

681 Weber, K. P. and Legge, R. L.: Community-Level Physiological Profiling, in *Bioremediation*,
682 pp. 263–281, Humana Press., 2010.

683 Williams, C. J., Yamashita, Y., Wilson, H. F., Jaffe, R. and Xenopoulos, M. A.: Unraveling the
684 role of land use and microbial activity in shaping dissolved organic matter characteristics in
685 stream ecosystems, *Limnol. Oceanogr.*, 55(3), 1159–1171, doi:10.4319/lo.2010.55.3.1159,
686 2010.

687 Williams, C. J., Frost, P. C., Morales-Williams, A. M., Larson, J. H., Richardson, W. B.,
688 Chiandet, A. S. and Xenopoulos, M. A.: Human activities cause distinct dissolved organic
689 matter composition across freshwater ecosystems, *Glob. Chang. Biol.*, 22(2), 613–626,
690 doi:10.1111/gcb.13094, 2016.

691 Wilson, H. F. and Xenopoulos, M. A.: Effects of agricultural land use on the composition of
692 fluvial dissolved organic matter, *Nat. Geosci.*, 2(1), 37–41, doi:10.1038/ngeo391, 2009.

693 Wu, Z., Wu, W., Lin, C., Zhou, S. and Xiong, J.: Deciphering the origins, composition and

694 microbial fate of dissolved organic matter in agro-urban headwater streams, *Sci. Total*
695 *Environ.*, 659(163), 1484–1495, doi:10.1016/j.scitotenv.2018.12.237, 2019.

696 Xenopoulos, M. A., Barnes, R. T., Boodoo, K. S., Christina, C. D. A., Nu, D. B., Kothawala,
697 D. N., Pisani, O., Solomon, C. T., Spencer, R. G. M., Williams, C. J. and Wilson, H. F.: How
698 humans alter dissolved organic matter composition in freshwater : relevance for the Earth ' s
699 biogeochemistry, , 3, doi:10.1007/s10533-021-00753-3, 2021.

700 Yamashita, Y., Scinto, L. J., Maie, N. and Jaffé, R.: Dissolved Organic Matter Characteristics
701 Across a Subtropical Wetland's Landscape: Application of Optical Properties in the
702 Assessment of Environmental Dynamics, *Ecosystems*, 13(7), 1006–1019,
703 doi:10.1007/s10021-010-9370-1, 2010.

704

705 **Table caption**

706 **Table 1** – Selected properties and dominant classification of sampling sites

707 **Table 2** – Spectral properties (positions of maximum excitation (ex) and emission (em) peaks)
708 of the eight PARARAC components identified in this study, general description and dominant
709 sources based on previous studies.

710

711 **Figure caption**

712 **Figure 1** – Map of the Lake Geneva Basin and the ten independent catchments sampled
713 during this study.

714 **Figure 2** – Boxplots of (A) Chla, (B) SRP, (C) DIN, (D) DOC concentrations and (E) S_R values
715 and (F) BR in agro-urban (grey) and forest-grassland (white) streams. The box represents the
716 first and third quartile, the horizontal line corresponds to the median, the cross corresponds to
717 the average, and the error bars correspond to the maximum and minimum. Mann Whitney
718 unpaired t -test were used to test for statistical differences: ns represents not significant, *
719 $=p<0.05$, ** $=p<0.01$, *** $=p<0.001$, **** $=p<0.0001$.

720 **Figure 3** – Boxplots of F_{Max} values of PARAFAC components in agro-urban (grey) and forest-
721 grassland (white) streams. The box represents the first and third quartile, the horizontal line
722 corresponds to the median, the cross corresponds to the average, and the error bars
723 correspond to the maximum and minimum. Mann Whitney unpaired t -test were used to test for
724 statistical differences: ns represents not significant, * $=p<0.05$, ** $=p<0.01$, *** $=p<0.001$, ****
725 $=p<0.0001$.

726 **Figure 4** – PCA biplot, including loadings plot for the input variables and scores plot for
727 stations. Markers are shaped according to the sampling period and colored according to a
728 gradient of human disturbance (defined as the sum of % croplands and % urban areas,
729 supplementary ordinal variable in the PCA).

730 **Figure 5** – Boxplots of (A) BDOC concentrations, (B) constant decay k , (C) STRC and (D)
731 LTRC pools in agro-urban (grey) and forest-grassland (white) streams. The box represents the
732 first and third quartile, the horizontal line corresponds to the median, the cross corresponds to
733 the average, and the error bars correspond to the maximum and minimum. Mann Whitney
734 unpaired t -test were used to test for statistical differences: ns represents not significant, *
735 $=p<0.05$, ** $=p<0.01$, *** $=p<0.001$, **** $=p<0.0001$.

736 **Figure 6** - Relationships between (A) BDOC, (B) decay constants and (C) the size of the STRC
737 pools with the sum of initial F_{Max} values of C6, C7, and C8 components.

738 **Figure 7** – Response ratio of PARAFAC components during incubation experiments with $t_f =$
739 day 28 and $t_0 =$ day 0. Grey bars represent threshold of significance above or below which
740 significant production or consumption of component was identified. See text for details.

741 **Figure 8** – Boxplots of (A) AA, (B) CAR, and (C) C&AA consumption in agro-urban (grey) and
742 forest-grassland (white) streams. The box represents the first and third quartile, the horizontal
743 line corresponds to the median, the cross corresponds to the average, and the error bars
744 correspond to the maximum and minimum. Mann Whitney unpaired t -test were used to test for

745 statistical differences: ns represents not significant, * = $p < 0.05$, ** = $p < 0.01$, *** = $p < 0.001$, ****
746 = $p < 0.0001$.

747 **Figure 9** – Relationships between BR and (A) DOC concentrations, (B) the sum of initial F_{Max}
748 values of C6, C7, and C8 components, and (C) initial F_{Max} values of C1 component

749

750 Table 1

751

Site	Area (km ²)	Mean elevation (masl)	Strahler order	Forest (%)	Croplands (%)	Urban areas (%)	Classification
1 - La Combe	39	1241	2	73	3	1	Forest-grassland
2 - Le Boiron	11	692	2	62	36	1	Forest-grassland
3 - Le Grand Curbit	14	614	2	24	70	4	Agro-urban
4 - La Venoge	228	696	4	31	60	6	Agro-urban
5 - La Mèbre	21	597	3	18	38	43	Agro-urban
6 - La Sorge	12	595	3	24	65	11	Agro-urban
7 - La Dranse	638		4	33	14	5	Forest-grassland
8 - Le Rhône	5238	2124	7	23	2	3	Forest-grassland
9 - La Veveyse	65	1105	5	45	20	6	Forest-grassland
10 - La Paudèze	16	775	4	33	40	25	Agro-urban

752

753 Table 2

754

Component	Max ex (nm)	Max em (nm)	Description & dominant sources
C1	<270	424	Widespread humic-like fluorophore, terrestrial ^{a,b} and/or photoproduced ^c .
C2	<270 (330, 380)	498	Fulvic-like fluorophore, widespread, terrestrial origin ^{d,e} .
C3	<270 (355)	438	Humic-like fluorophore, widespread, terrestrial origin ^d .
C4	320	402	Low molecular weight humic-like fluorophore, related to agriculture ^{a,b,e} .
C5	300	336	Protein-like fluorophore associated with biological production ^f .
C6	<270	372	Anthropogenic humic-like fluorophore related to algal ^g or bacterial ^f production in urban areas ^{e,g} .
C7	275	332	Tryptophan-like fluorophore, indicative of autochthonous production ^{b,c} .
C8	270	304	Tyrosine-like fluorophore, indicative of autochthonous production ^{b,c} .

^a Stedmon & Markager, 2005; ^b Yamashita et al., 2010; ^c Massicote & Frenette 2011; ^d Graeber et al., 2012;

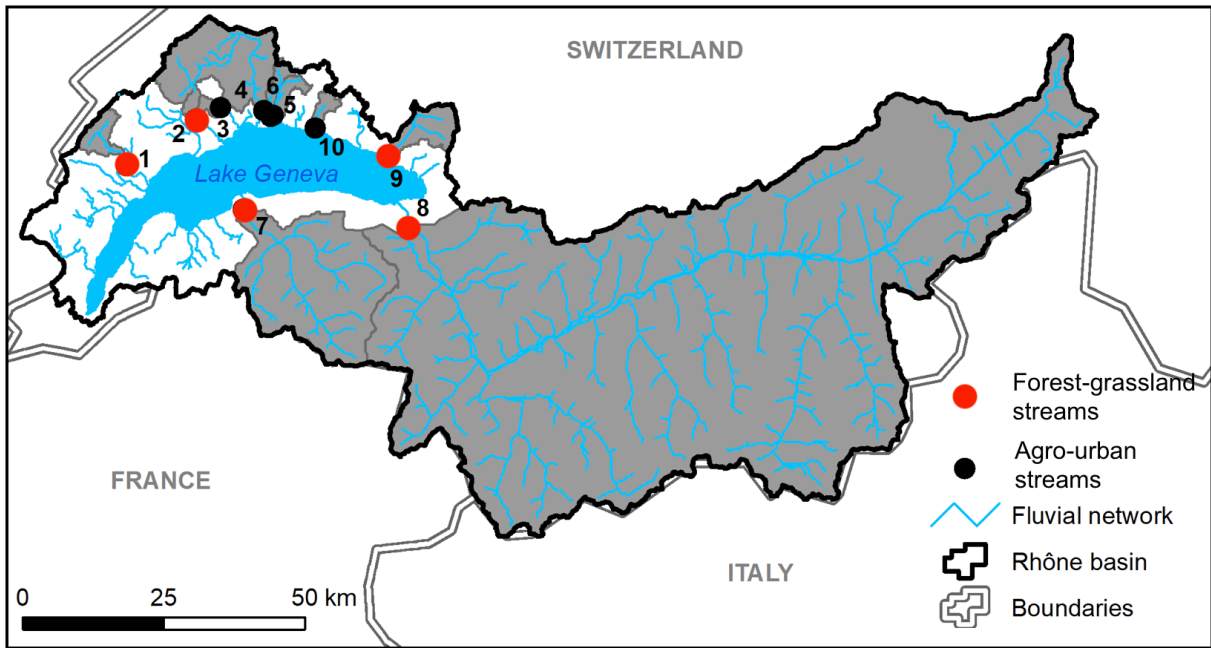
^e Lambert et al., 2017; ^f Stedmon et al., 2011; ^g Williams et al., 2016.

755

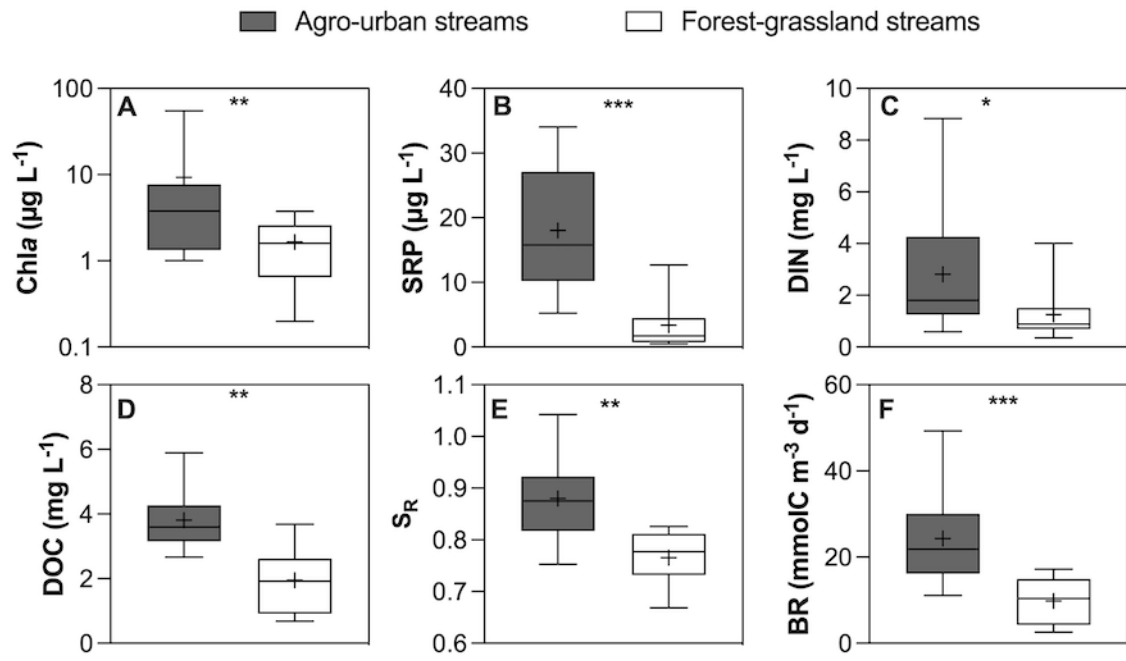
756 Figure 1

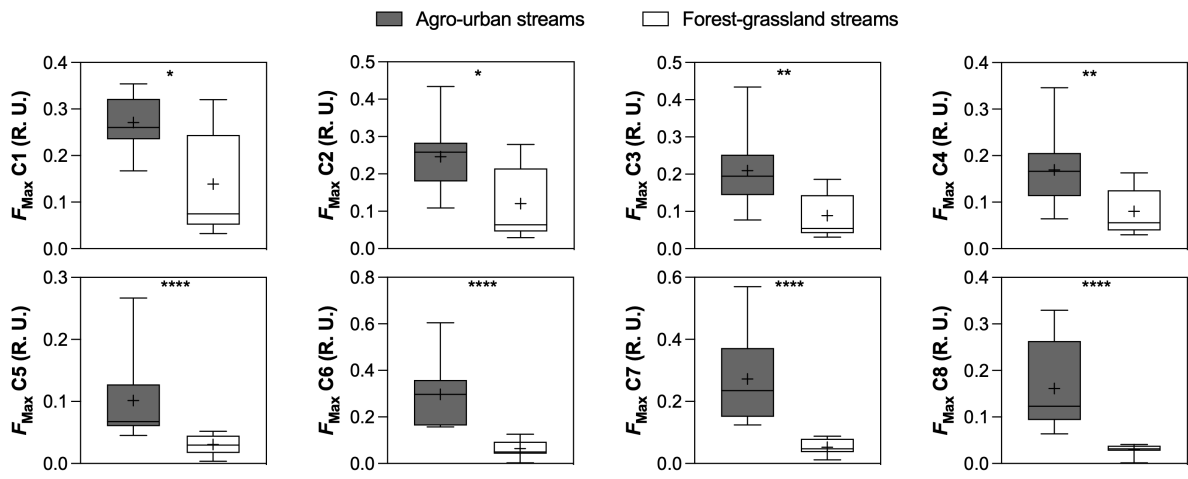
757

758

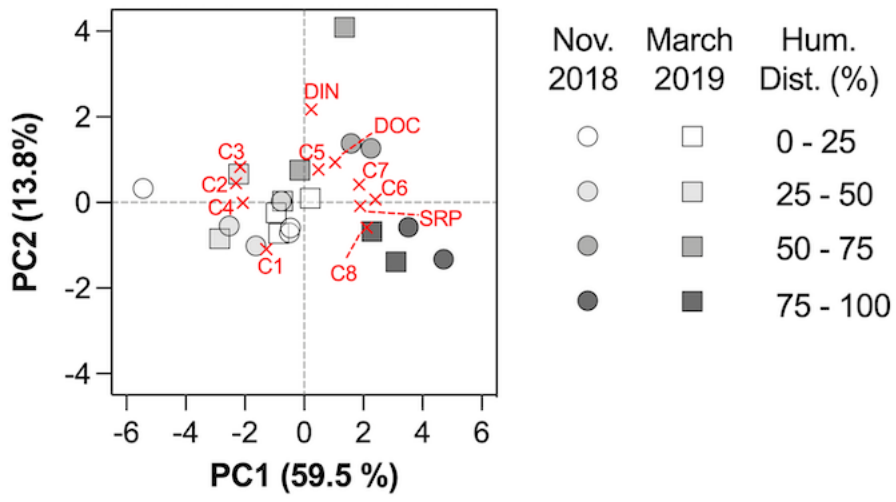


759

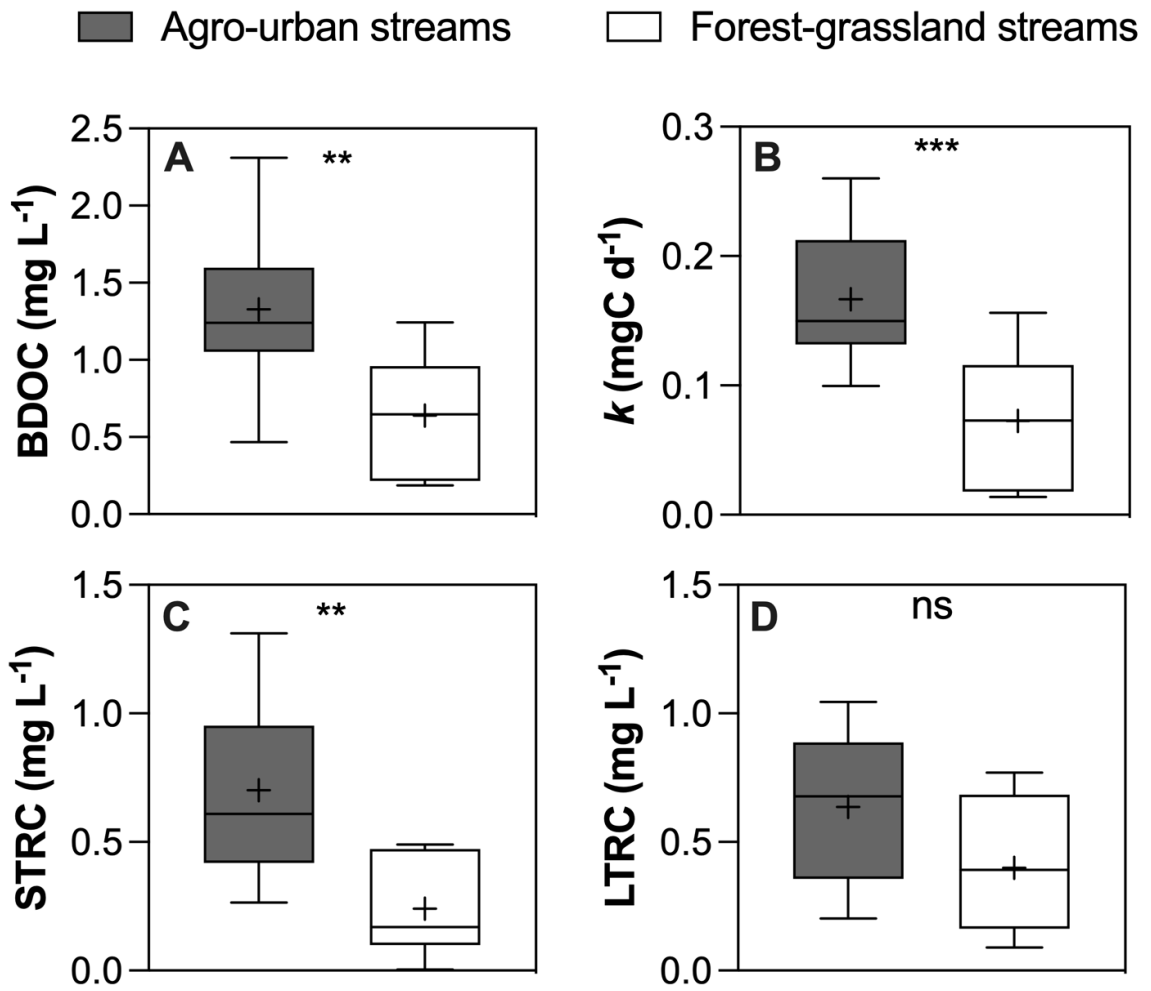




764 Figure 4

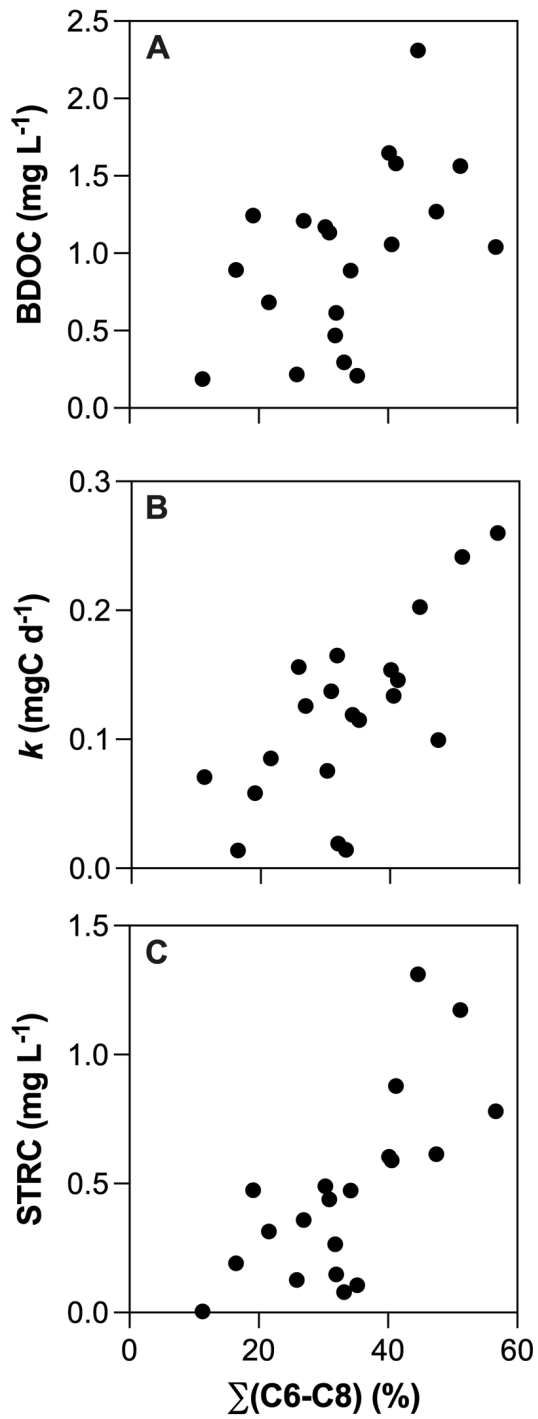


765



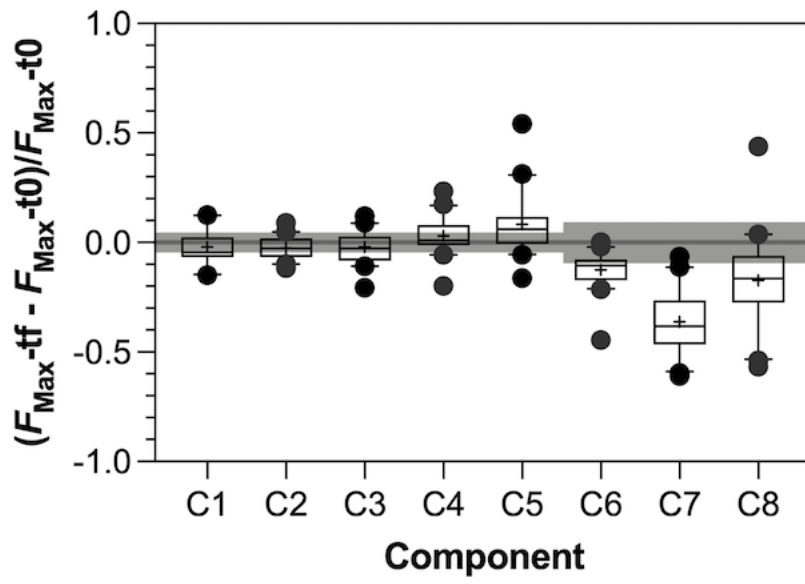
768 Figure 6

769



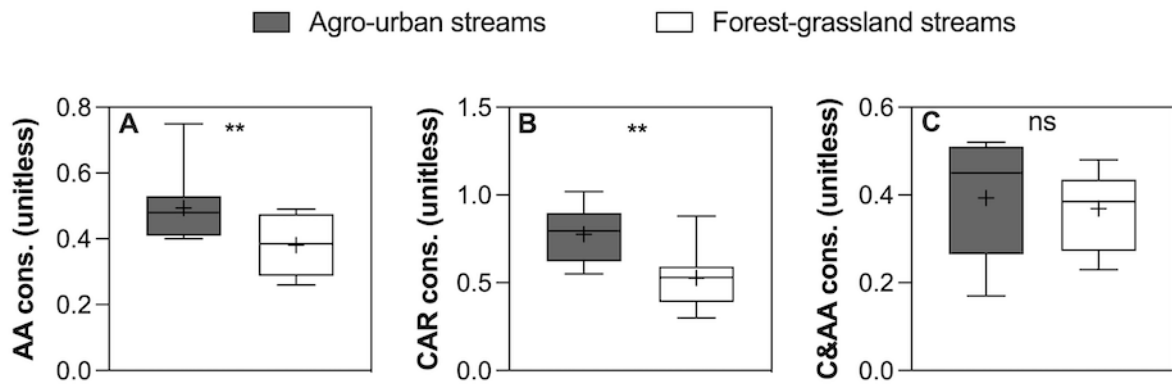
770

771 Figure 7



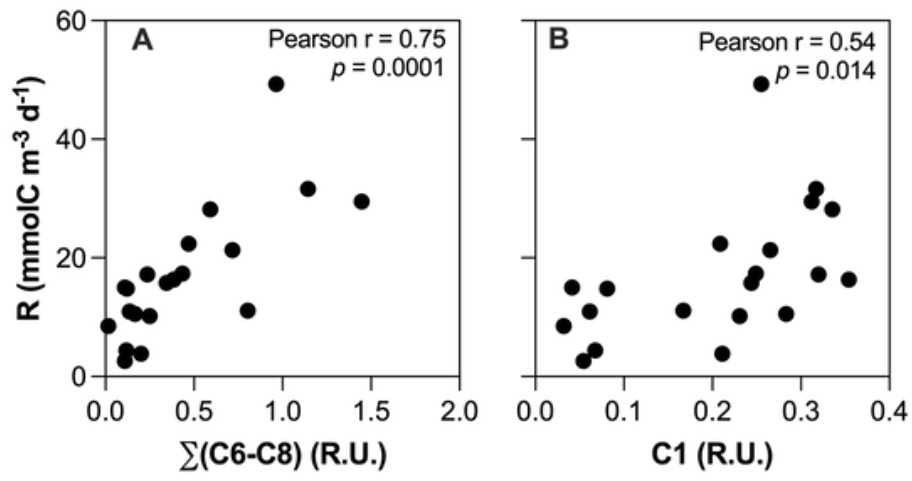
772

773 Figure 8



774

775 Figure 9



776